ELSEVIER

Polymer 41 (2000) 7843–7854

polymer

The kinetics of α and β transcrystallization in fibre-reinforced polypropylene

E. Assouline[a,b], S. Pohl[c], R. Fulchiron[d], J.-F. Gérard[d], A. Lustiger[e], H.D. Wagner[b], G. Marom[a,*]

[a]*Casali Institute of Applied Chemistry, Givat Ram Campus, The Hebrew University of Jerusalem, Jerusalem 91904, Israel*
[b]*Department of Materials and Interfaces, The Weizmann Institute of Science, Rehovot 76100, Israel*
[c]*IKP, Universität Stuttgart, Stuttgart D-70511, Germany*
[d]*UMR-CNRS 5627, L.M.M. INSA Lyon, L.M.P.B. Université Lyon I, Villeurbanne 69622 Cedex, France*
[e]*Exxon Research and Engineering, Route 22 East, Annandale, NJ 08801, USA*

Received 11 October 1999; received in revised form 17 December 1999; accepted 2 February 2000

Abstract

The kinetics of α (monoclinic) and β (hexagonal) transcrystallization of isotactic polypropylene on aramid Kevlar 149 fibres, glass fibres and high modulus carbon fibres was investigated under isothermal and gradient cooling conditions. No difference was found between growth rates of bulk spherulites and transcrystalline layers, and Hoffman's theory led to the same results in both cases. Regarding α transcrystallization, a transition between regimes II and III occurred near 137°C and the ratio of the slopes of the two regimes was close to the theoretical value of 2. Regarding β transcrystallization, only regime II was exhibited in the temperature range studied. However, the induction time for transcrystallization was strongly influenced by the type of fibre, which in turn—based on Ishida's approach—resulted in variations in free energy differences at the fibre–crystallite interface for various fibres and bulk polypropylene. The respective values were 1.3, 1.5 and 2.1×10^{-3} J m^{-2} for Kevlar 149 fibres, high modulus carbon fibres than in polypropylene, showing that α crystallization is more likely to occur in Kevlar 149 fibres and high modulus carbon fibres and bulk polypropylene. Gradient-thermal measurements were performed for α transcrystallinity which allowed estimation of the activation energy of transcrystallization for the different composites. Activation energies of transcrystallinity promoted on Kevlar 149 and high modulus carbon fibres were found higher than the activation energy for bulk crystallization.

Keywords: Polypropylene; α and β transcrystallization; Isothermal crystallization

1. Introduction

Isotactic polypropylene (iPP) based materials are often reinforced by fibres, such as glass, aramid and carbon in order to improve their mechanical properties. Under certain conditions, the fibres induce a relatively high crystal nucleation density on their surface. Therefore the matrix spherulites grow from the fibre in the radial direction only, to produce a cylindrical layer of crystallinity, termed transcrystallinity. The strong orientation of the transcrystalline (tc) layer is expected to have different effects on the mechanical properties of composite materials, including a significant improvement of the longitudinal ultimate strength and modulus. An interesting aspect of transcrystallization is its growth kinetics since it influences the thickness of the tc layer, which in turn will affect the mechanical properties.

Several theories of crystallization kinetics have been proposed for semi-crystalline polymers. Using the example of polyethylene [1,2], Hoffman defined three crystallization regimes. Each regime is characterized by the way the chains are deposited on the substrate and by the relation between the spherulite growth rate and the nucleation rate. Another approach to nucleation concerns induction time, which is the delay between the time zero (when the temperature has reached the chosen crystallization temperature) and the time of the onset of nucleation. According to Ishida [3], this parameter is connected to the nucleation rate and it enables the calculation of thermodynamic parameters.

It is important to study the kinetics of transcrystallization as a function of both crystallization temperature and the reinforcing fibre. Indeed, these two parameters play a crucial role in the kinetics and in the morphology of the tc layer. The theories and techniques developed for the crystallization of matrices have been used also for

* Corresponding author. Tel.: +972-2-658-5898; fax: +972-2-652-8250.
E-mail address: gadm@vms.huji.ac.il (G. Marom).

0032-3861/00/$ - see front matter
PII: S0032-3861(00)00113-0

transcrystallization. Hoffman's regime theory was applied to different systems: in microcomposites of Kevlar 49 fibre/iPP [4] and of high modulus carbon fibre/iPP [5], the temperature range for isothermal crystallization (121–135°C and 126–135°C, respectively) permitted the observation of only one crystallization regime. In polytetrafluoroethylene (PTFE)/iPP fibre system [6], the tc layer exhibited a transition from regime III to regime II at 137°C. An induction time approach allowed calculation of the interfacial free energy difference. A recent work [7] compared the nucleating ability of different fibres by measuring the interfacial free energy difference functions in the different iPP based systems. This was based on the calculation of nucleation density of iPP at the fibre surface at different crystallization temperatures. According to this study, transcrystallization is most likely to occur on PTFE since it exhibits the lowest interfacial free energy difference. Both the thermal expansion coefficient and the surface morphology seem to play also a key role in the nucleation of a tc layer. Gradient thermal measurements allowed calculation of the activation energy of transcrystallization for carbon fibre/J-1 polymer [8,9] and for aramid fibre and carbon fibre/nylon 66 composites [10]. In glass fibre/iPP microcomposites [11], no transcrystallinity was observed but a strong nucleating effect in the matrix was noticed. Crystallization growth rates in the bulk and at the tc interface were found to be similar [5].

Whereas the influence of different fibres has been extensively studied in polypropylene based composites, the influence of the form of matrix crystallinity has been relatively ignored. Indeed, iPP is polymorphic and it is therefore interesting to compare transcrystallization of its three forms. In general, for iPP-based systems, α monoclinic transcrystallinity has been mainly investigated [4–7]. Less work has been carried out concerning β hexagonal crystalline interfaces induced by nucleating agents [12] or promoted by shearing stress [13,14], and even less work exists for γ orthorhombic tc layers [15]. No kinetics data for β and γ transcrystallization were found in the literature.

The objectives here are to study the α and β transcrystallization kinetics at the iPP–fibre interface (the study of the γ kinetics has been made impossible by the fact that the device used to generate γ tc layer did not allow observation in real time of the inside of the crystallization cell [15]). Microcomposites of high modulus carbon fibre/iPP, Kevlar 149 fibre/iPP and glass fibre/iPP were examined. Three approaches were considered in this study: the Hoffman's regime theory, the induction time approach and gradient-thermal measurements.

2. Experimental

2.1. Sample preparation

Isotactic polypropylene of number average molecular weight $M_n = 43,700$ and weight average molecular weight $M_w = 212,500$ was supplied by Exxon (MFR = 12). Aramid Kevlar 149 fibres (KF) of diameter 12 μm and high modulus carbon fibres (HMCF) of diameter 8 μm were provided by DuPont. Glass fibres (GF) from Vetrotex International had a diameter 14 μm. Red quinacridone, provided by Hoechst Celanese, was used as a β nucleating agent. Since KF and HMCF exhibit an α nucleating ability, they were used without prior treatment. Uncoated GF generally do not induce transcrystallization except under shear. Therefore they were coated with red quinacridone to promote a β tc layer. The pigment was dissolved in dimethyl formamide (at about 0.1% in weight). The fibres were steeped in this suspension for 4 h and then dried overnight in an oven at 160°C.

Single fibre-composites were prepared as follows: one fibre was placed on a glass slide. A piece of iPP (surface: about 1 cm^2; thickness: 80–150 μm) was placed on the fibre. A thin glass slide prevented the molten iPP from adhering to the upper plate of the hot-stage. Using the heat-controller Mettler FP80, the temperature was raised up to 204°C over a period of 3 min to erase the previous thermal history of the sample. When the polypropylene melted, it surrounded the whole portion of the fibre located under the upper slide.

2.2. Measurements

A Nikon optical microscope equipped with cross polarizers permitted viewing of the inner cell of the Mettler FP82 hot-stage and crystallization. It was connected to a Sony video camera and to a picture printer. Using a calibration of the printed image, the radius of the transcrystalline layer was measured at regular time intervals, until 1 h or until the obscuring of the tc layer by the abundant presence of spherulites above and below the fibre.

Under isothermal conditions, the crystallization temperature ranged from 112 to 140°C for KF/iPP and HMCF/iPP microcomposites and from 126 to 152°C for GF/iPP systems. A fast cooling (−20°C min^{-1}) was used to reach the isothermal crystallization temperature. The growth rate (G) of the tc layer was calculated as the slope of the linear part of the plot of the thickness of the tc layer versus time. In order to get significant values, the experiments were repeated 5–9 times. The average and the standard deviation of the growth rate were calculated for each set of measurements. The values of G as a function of time were used in Eq. (1) in order to determine the Hoffman's regime transition and the slopes of the two linear areas. For treated GF based microcomposites, the temperature was raised to 160°C at the end of the experiment to melt the β phase of the interface and to estimate the thickness of the α phase in the tc layer.

The induction time was taken as the onset time for transcrystallization. It is noted that the nucleation rate was too high to be estimated by counting the nuclei at the interface. Thus it was impossible to estimate the induction time by

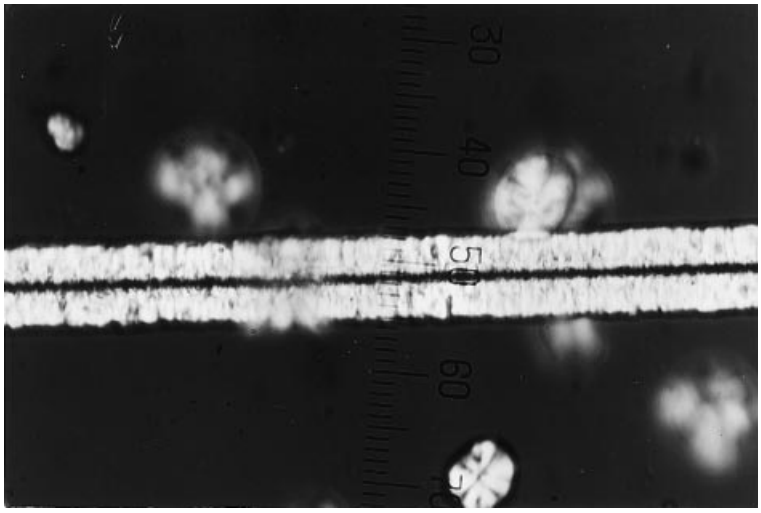

Fig. 1. A photograph of an α transcrystalline layer in HMCF/iPP.

extrapolating the nucleation density to the time axis. The values of induction time as function of temperature were used in Eq. (3) in order to calculate the product of the three surface energy terms.

In gradient-thermal conditions, the microcomposite was non-isothermally crystallized at different cooling rates (from -1 to -20°C min^{-1}). The temperature at the maximum of the crystallization rate T^* was taken as the highest slope of the recording of the depolarization of light passing through the vicinity of the fibre as a function of the temperature using light analyser. The activation energy was calculated from the slope of the plot of ln(cooling rate) versus $1/T^*$ (according to Eq. (8)).

3. Results

3.1. α Transcrystallization

A typical α tc layer developed on a HMCF in an α iPP matrix is shown in Fig. 1. The thickness of such an interface is greatly dependent on time and on crystallization temperature as shown for KF/iPP (Fig. 2), HMCF/iPP (Fig. 3) and GF/iPP (Fig. 4) composites. It should be stressed that an α tc layer is first promoted on the β-treated GF at higher temperatures, as will be explained later. From these measurements, the growth rate of the tc layer was plotted versus crystallization temperature in Fig. 5 for the three investigated systems. According to kinetics theories, G can be expressed by Eq. (1) [1,2,16,17]:

$$G = G_0 \exp[-U^*/\mathrm{R}(T - T_{\inf}]\exp[-K_g/T(\Delta T)f] \quad (1)$$

where G_0 is a pre-exponential factor containing quantities independent of the temperature; $U^* = 6280$ J is a universal constant, characteristic of the activation energy of chain motion in the melt; $T_{\inf}$ is the theoretical temperature at which any motion associated with viscous flow or reptation ceases, $T_{\inf} = T_g - 30$; ΔT is the undercooling, $\Delta T = T_m^0 - T$ (T_m^0 is the equilibrium melting point); f is a correcting factor, $f = 2T/(T_m^0 + T)$; and K_g is the nucleation constant, K_g of regime II is half the value of the nucleation constant of regime I and III:

$$K_{g(I)} = 4b_0\sigma\sigma_e T_m^0/(\Delta h_f)\mathrm{k} \quad (2)$$

where b_0 is the thickness of the new layer; σ is the lateral surface free energy; σ_e is the fold surface free energy; Δh_f is the enthalpy of fusion; and k is the Boltzmann constant. The values of a number of these parameters are reported in Table 1.

Using Eq. (1), $\log G + U^*/2.303\mathrm{R}(T - T_{\inf})$ was plotted versus $1/T(\Delta T)f$ in Fig. 6. Two linear parts are displayed: the change of the slope occurs at 136.6°C and the slope ratio is 1.92. From the slopes, it was estimated that $\sigma\sigma_e = 7.89 - 8.36 \times 10^{-4}$ J m^{-4}.

In Fig. 7, induction times are displayed versus crystallization temperature for KF and HMCF based microcomposites. Induction times could not be measured below 126°C for KF/iPP composites and below 130°C for HMCF/iPP composites because transcrystallization started before the

Table 1
Essential parameters for the kinetics study of the α and β transcrystallization according to Hoffman's theory

Parameter	α Phase	β Phase
T_m^0 (K)	458[a,b]	449K[b]
Δh_f (MJ m^{-3})	196[a–c]	177[b]
$T_{\inf}$ (K)	231.2[a]	231.2[a]
a_0 (Å)	5.49[a,b]	6.36[b]
b_0 (Å)	6.26[a,b]	5.51[b]

[a] Data taken from Ref. [16].
[b] Data taken from Ref. [19].
[c] Data taken from Ref. [7].

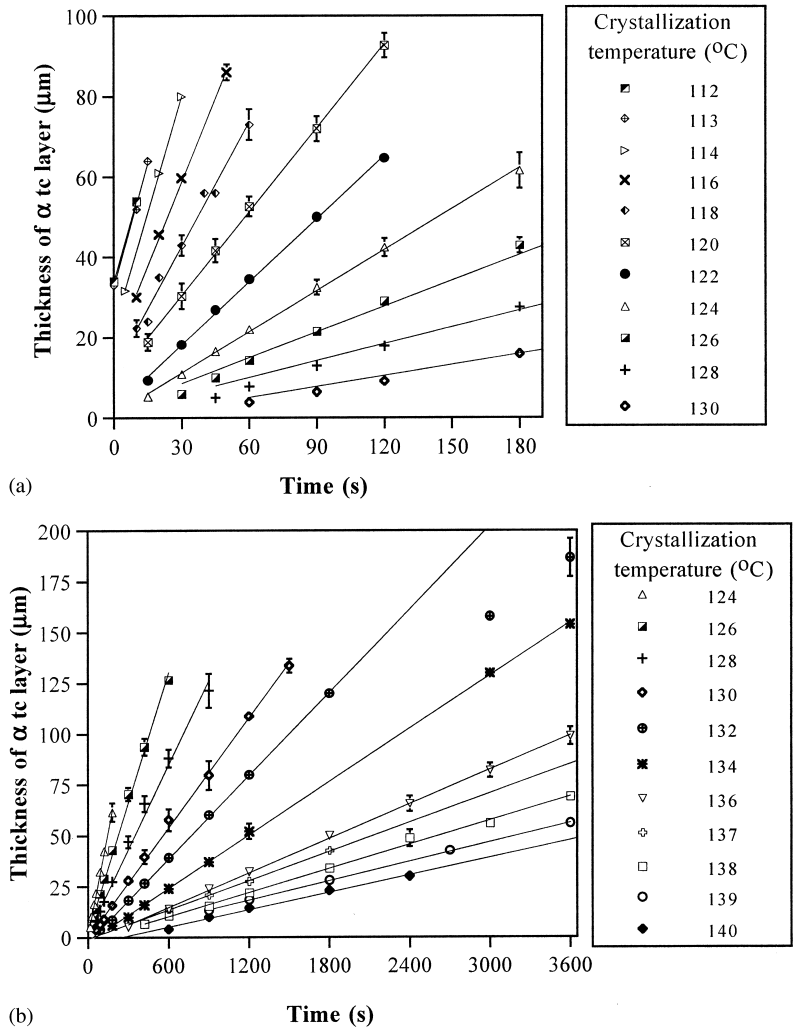

Fig. 2. Kinetics of α transcrystallization in KF/iPP: (a) initial stage (3 min); (b) in the full time range.

isothermal crystallization temperature was reached. According to Ishida's assumption [3], at a given temperature T, the number of nuclei per unit area is a constant K because the nucleation rate $I(T)$ and the induction time $t_i(T)$ evolve in an opposite way: when the crystallization temperature increases, the induction time increases and the nucleation rate decreases. Thus:

$$I(T) \times t_i(T) = K \tag{3}$$

where [17]

$$I(T) = I_0 \exp(-U^*/\mathrm{R}(T - T_{\inf}))\exp(-\Delta G^*/\mathrm{k}T) \tag{4}$$

ΔG^* is the critical excess free energy due to the creation of a nucleus and is given by [18]:

$$\Delta G^* = \frac{16\sigma\sigma_e\Delta\sigma T_m^{0^2}}{\Delta T^2 f^2 \Delta h_f^2} \tag{5}$$

$\Delta\sigma$ is the free energy difference at the fibre–crystallite interface and measures the amount of energy necessary to create a new fibre–crystallite interface. From Eqs. (3)–(5), it is deduced that a plot of $\log(1/t_i(T)) + U^*/2.303\mathrm{R}(T - T_{\inf})$ versus $1/(T\Delta T^2 f^2)$ leads to a straight line whose slope is:

$$\frac{-16T_m^{0^2}}{2.303 \times \mathrm{k}\Delta h_f^2}\sigma\sigma_e\Delta\sigma \tag{6}$$

Fig. 8 displays this plot for HMCF/iPP, KF/iPP composites and for iPP. The points could be actually fitted with a straight line with a good correlation coefficient for both systems. From the slopes, the values of $\sigma\sigma_e\Delta\sigma$ were calculated. $\Delta\sigma$ was then estimated using Eqs. (2) and (6) and the data in Table 2. An approximation proposed by Hoffman was used [1] to estimate σ (Eq. (7)):

$$\sigma = \Delta h_f \frac{a_0}{2}\frac{l_b}{l_u}\frac{1}{C_\infty} \tag{7}$$

where l_b is the bond length (0.154 nm), l_u is the projected length per atom (0.1084 nm) and C_∞ is the characteristic ratio (5.7). It was found that $\sigma = 13.4 \times 10^{-3}$ J m^{-2} and consequently, $\sigma_e = 60.6 \times 10^{-3}$ J m^{-2} (these values are consistent with results published in the

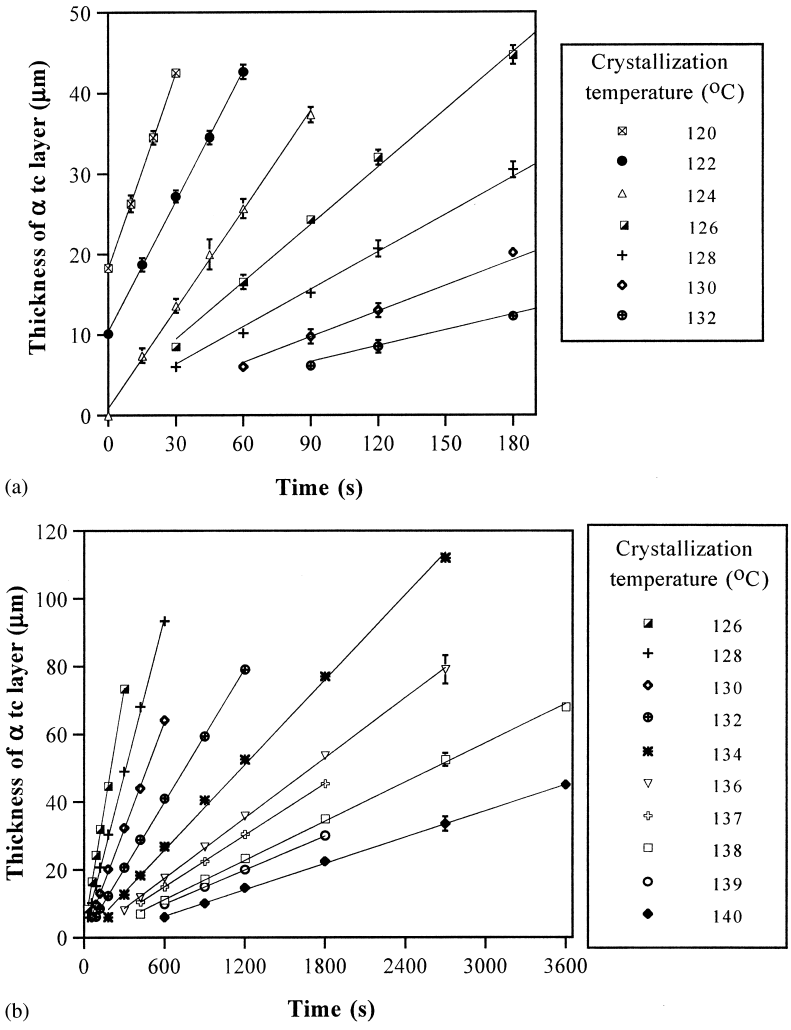

Fig. 3. Kinetics of α transcrystallization in HMCF/iPP: (a) initial stage (3 min); (b) in the full time range.

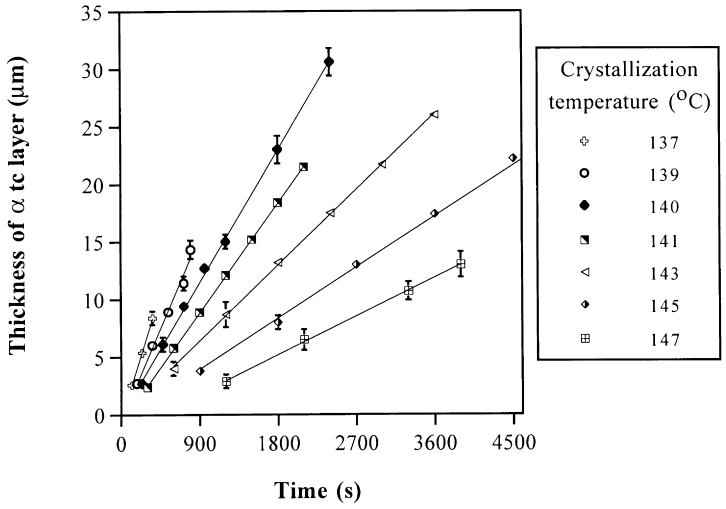

Fig. 4. Kinetics of α transcrystallization in GF/iPP.

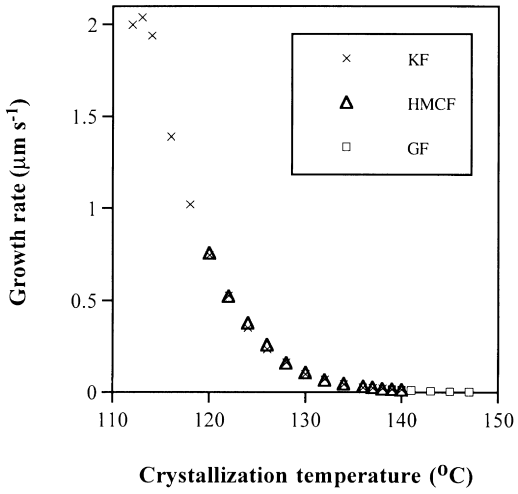

Fig. 5. The growth rate of α transcrystalline layers versus temperature.

literature [19] $\sigma = 11 \times 10^{-3}$ J m^{-2} and σ_e in the range 40–230 $\times 10^{-3}$ J m^{-2}).

Gradient-thermal crystallization was performed at different cooling rates. The intensity of depolarized light was plotted versus temperature (Figs. 9–11). It enabled the determination of the temperature of the highest crystallization rate $T^{\prime,*}$, which is related to the cooling rate Q by an Arrhenius type relation [20]:

$$\ln Q = \frac{1.052E_a}{RT^*} \quad (8)$$

where E_a is the activation energy of crystallization. The plots of $1/T^*$ as a function of ln Q lead to straight lines, as shown for neat iPP matrix and for KF/iPP and HMCF/iPP composites (Fig. 12). Based on the correlation coefficients, the level of significance of the linear regressions is higher than 99%. The values of activation energies are proportional to the inverse of the slopes and are reported in Table 3.

Table 2
Surface energies in α iPP-based systems

System	$\sigma\sigma_e\Delta\sigma$ (10^{-6} J^3 m^{-6})	$\sigma\sigma_e$ (10^{-4} J^2 m^{-4})	$\Delta\sigma$ (10^{-3} J m^{-2})
HMCF/iPP	1.27	8.1–8.4	1.51–1.56
KF/iPP	1.08	8.1–8.4	1.29–1.33
iPP (spherulites)	1.73	8.1–8.4	2.06–2.14

Table 3
Activation energy for different α iPP-based systems

Sample	E_a (kJ mol^{-1})
iPP (matrix)	206
HMCF/iPP (tc layer)	240
KF/iPP (tc layer)	265

3.2. β Transcrystallization

A β tc layer was induced by GF in an α iPP matrix and is shown in Fig. 13. Although the fibres were coated with a β nucleating agent, a pure β transcrystalline layer was never obtained at any isothermal crystallization temperature. The border between the α and the β forms ("the α/β border") displays a "saw tooth" shape (Fig. 14) due to the fact that β crystallization proceeds at a significantly faster rate than α [21]. Until 138°C, there is a mixture of α and β phases in the tc layer; transcrystallization starts with the α phase which only later evolves to a β form. The higher the temperature, the higher the amount of α phase (Fig. 15). More strikingly, the tc layer was only of α form above 138°C.

The thickness of the β tc layer was evaluated from the α/β border for several crystallization temperatures (Fig. 16) and consequently the growth rate was calculated as presented in Fig. 17, where a comparison with the growth rate of α transcrystallinity is made. Following Hoffman's

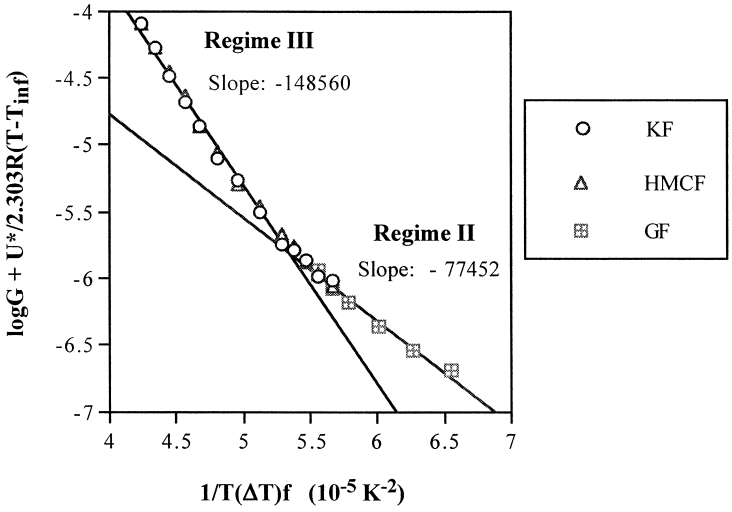

Fig. 6. A plot of log $G + U^*/2.303R(T - T_{inf})$ versus $1/T(\Delta T)f$ (according to Hoffman's theory) for the α transcrystalline layer in iPP based composites.

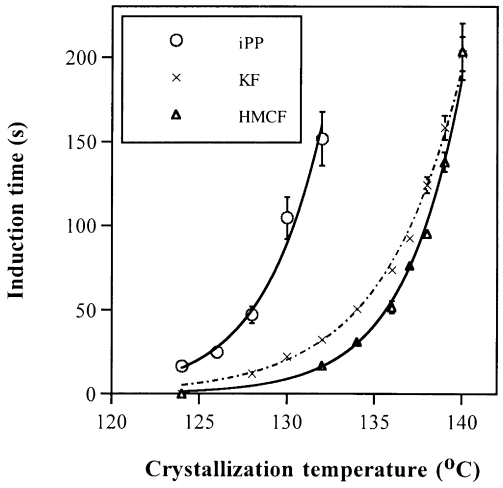

Fig. 7. The induction time of α transcrystallization in iPP-based composites versus crystallization temperature.

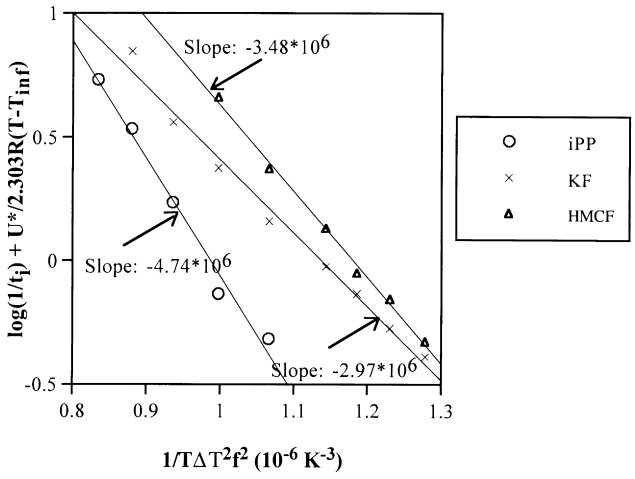

Fig. 8. A plot of $\log(1/t_i) + U^*/2.303R(T - T_{inf})$ against $1/T(\Delta Tf)^2$ (according to Ishida's theory) for the α transcrystalline layer in iPP-based composites.

theory, the plot of $\log G + U^*/2.303R(T - T_{inf})$ against $1/T(\Delta T)f$ led to a single straight line whose slope resulted in $\sigma\sigma_e = 11.4 \times 10^{-4}$ J^2 m^{-4} (Fig. 18).

Using Eq. (7), it was found that $\sigma = 14 \times 10^{-3}$ J m^{-2} and consequently that $\sigma_e = 82 \times 10^{-3}$ J m^{-2} (which agrees with the range of values found in the literature [19] $\sigma_e = 35–112 \times 10^{-3}$ J m^{-2}).

4. Discussion

According to the objectives of this study, the focal point of the discussion is the comparison of the kinetics of transcrystallization with that of bulk spherulitic crystallization.

4.1. α Transcrystallization

Under isothermal crystallization conditions, the main difference between bulk crystallization and transcrystallization is manifested in longer induction times for the former (Fig. 7). That difference, however, diminishes with the degree of supercooling. Thus, at lower crystallization temperatures, the growth of the tc layer becomes rapidly limited by impinging spherulites. Indeed, at lower crystallization temperatures, the induction time difference between bulk- and transcrystallization is reduced while the number of spherulites and their growth rate increase (Figs. 2–4).

The effect of the fibre is most evident during the nucleation stage, which is expected to be most sensitive to the nature of the fibre surface. It is seen that the induction time for transcrystallization is shorter when promoted by HMCF than by KF, suggesting that the surface of the HMCF offers a higher concentration of nucleation sites.

However, as anticipated, the fibre does not influence the kinetics of crystallization; for HMCF, KF and treated-GF reinforced composites identical transcrystallization growth

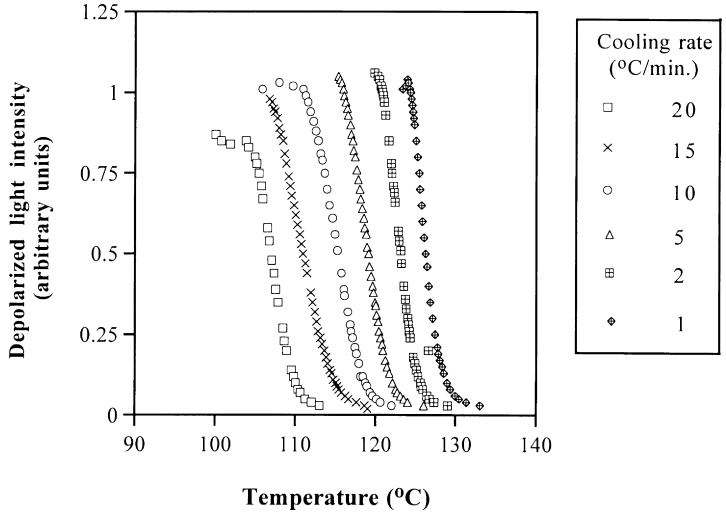

Fig. 9. Depolarized light intensity versus temperature for different cooling rates for neat iPP matrix.

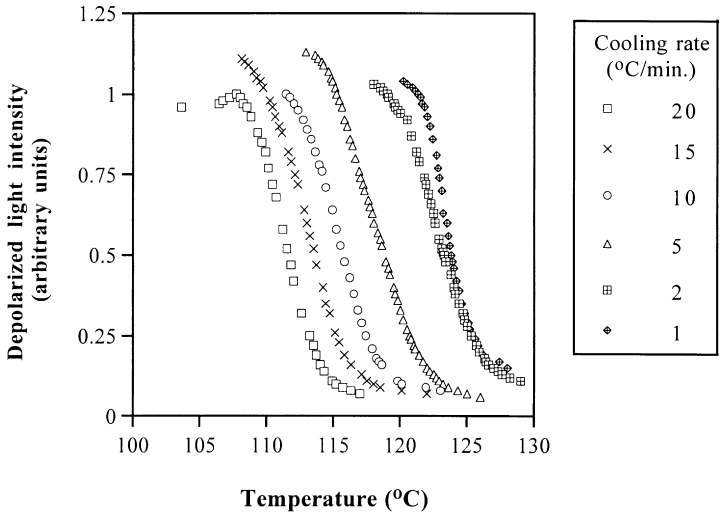

Fig. 10. Depolarized light intensity versus temperature for different cooling rates for KF/iPP transcrystallinity.

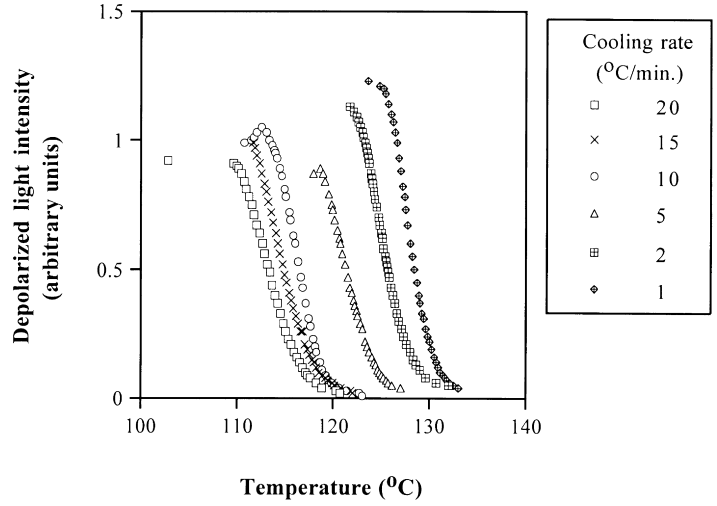

Fig. 11. Depolarized light intensity versus temperature for different cooling rates for HMCF/iPP transcrystallinity.

rates were exhibited (within experimental error). This finding confirms previous results [7] showing that the tc growth rate is unaffected by the fibre type and that the growth rate of transcrystallization is supposed to reflect matrix properties. Yet, because nucleation is fibre controlled, the ability to form a tc layer is dominated by the nature of the fibre [6]; some fibres, e.g. KF and HMCF, promote transcrystallization while others, e.g. untreated GF, do not. In addition, the shape of the tc layer depends on the fibre surface topography. Accordingly, a helical defect along KF [22] results in a tc helix (Fig. 19) while the parallel growing tc front on HMCF results in a much more uniform tc layer (Fig. 1).

The kinetics of transcrystallization is identical to that of bulk crystallization both in terms of growth rate and growth regimes in Hoffman's model. A maximum in growth rate is observed at 113°C (Fig. 5), which is identical to the maximum rate of α crystallization of bulk iPP. In terms of Hoffman's model, the plot of $\log G + U^*/2.303\mathrm{R}(T - T_{\inf})$

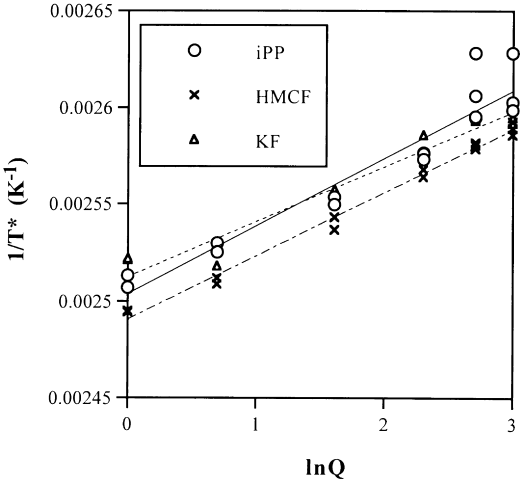

Fig. 12. $\ln Q$ versus $1/T^*$ for neat iPP matrix, KF/iPP and HMCF/iPP transcrystallinity.

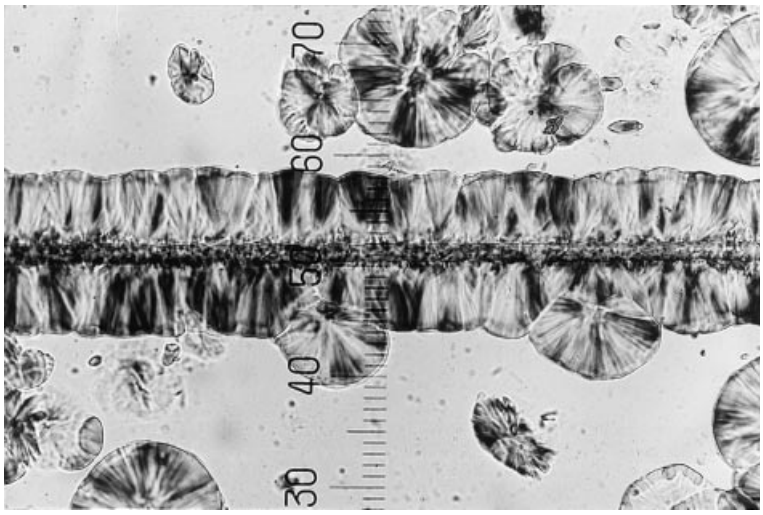

Fig. 13. A photograph of a β transcrystalline layer in GF/iPP at 128°C.

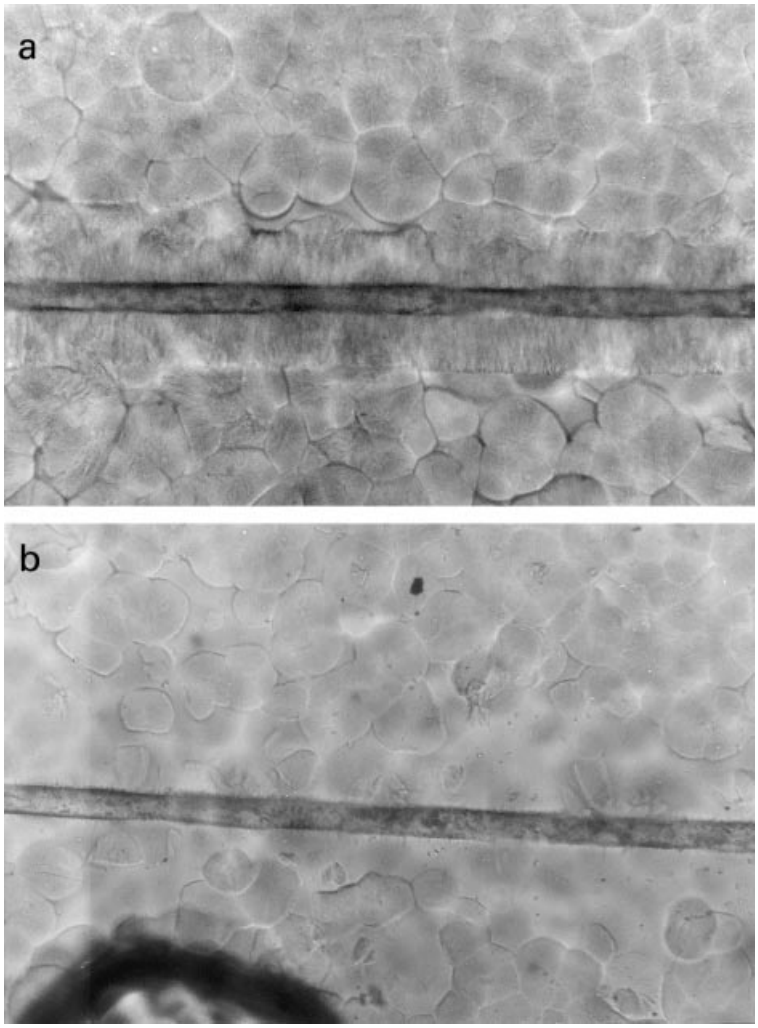

Fig. 14. A photograph of the α/β border in GF/iPP: (a) below the melting point of β iPP; (b) between the melting points of α and β iPP, showing the remaining "saw tooth" α phase.

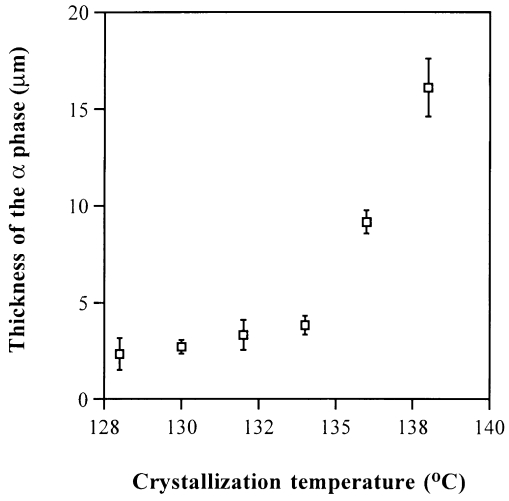

Fig. 15. The thickness of the α phase within the combined α/β transcrystalline layer on treated glass fibre versus crystallization temperature.

versus $1/T(\Delta T)f$ (Fig. 6) exhibits a significant slope change at 136.6°C corresponding with the regime III–regime II transition at 137°C as previously documented for the α crystallization of iPP [16]. The regime transition in transcrystallization is attributed to the same process change as in bulk crystallization, namely, a change from a regime of both tertiary and secondary nucleation (II) to a regime that is dominated by higher secondary nucleation (III).

The study of regime III is limited by the lower temperature bound at 113°C, producing the maximum rate of transcrystallization. Below this point the experimental error increases due to significantly shorter crystallization times. Similarly, the study of regime II–regime I transition is limited by an upper temperature bound, beyond which no transcrystallinity can develop, being 140°C for the HMCF and KF and 152°C for the GF-based composites. Therefore, despite the fact that α spherulitic low molecular mass iPP can exhibit a regime II–regime I transition near 148°C (ΔT 37°C) [23], regime I cannot be attained in the current system. Yet, in between those two limits, the results are consistent with Hoffman's theory and correspond with previous works published for spherulitic iPP, i.e. the regime III–regime II transition occurs at about 136.6°C which means that the supercooling is 48.4 K in agreement with the literature value of 48 K, and the slope ratio is 1.92 which is close to the theoretical value of 2 [16].

The observation that only in the nucleation stage does the fibre affect the crystallization kinetics is corroborated by a comparison of the free energy difference values. First, the values of $\sigma\sigma_e$ are in agreement with results found for a wide range of neat iPP matrices ($\sigma\sigma_e = 7.4$–7.9×10^{-4} J^2 m^{-4} [16]) and for α iPP tc layers ($\sigma\sigma_e = 7.32 \times 10^{-4}$ J^2 m^{-4} [7]). Then, the free energy differences $\Delta\sigma$ of the studied systems too are in agreement with the ones published by other authors: Wang et al. [7] found that $\Delta\sigma = 1.14 \times 10^{-3}$ J m^{-2} for high modulus carbon fibres. Moreover, the order of magnitude is also similar with values for other composites: $\Delta\sigma = 3.35 \times 10^{-3}$ J m^{-2} for Kevlar 49 reinforced composites, 0.75×10^{-3} J m^{-2} for PTFE fibres and 5.87×10^{-3} J m^{-2} for polyethylene terephthalate fibres. In the bulk it was found here that $\Delta\sigma = 2.1 \times 10^{-3}$ J m^{-2} (consistent with the value 1.23×10^{-3} J m^{-2} found for a different polypropylene matrix [7]). $\Delta\sigma$ is slightly lower for crystallization on KF than on HMCF, which means that transcrystallization is more likely to occur on KF than on HMCF. $\Delta\sigma$ is higher for bulk crystallization than for transcrystallization either on KF or on HMCF. Therefore transcrystallization on these fibres is preferred in comparison to bulk crystallization.

The activation energies of nucleation, calculated from the slope of the staight line plot of ln Q versus $1/T^*$ (Fig. 12), are different for bulk and transcrystallization (Table 3). In this case, the activation energy for nucleation of iPP of 206 kJ mol^{-1} is lower than those of HMCF/iPP (240 kJ mol^{-1}) and KF/iPP (265 kJ mol^{-1}). Although the

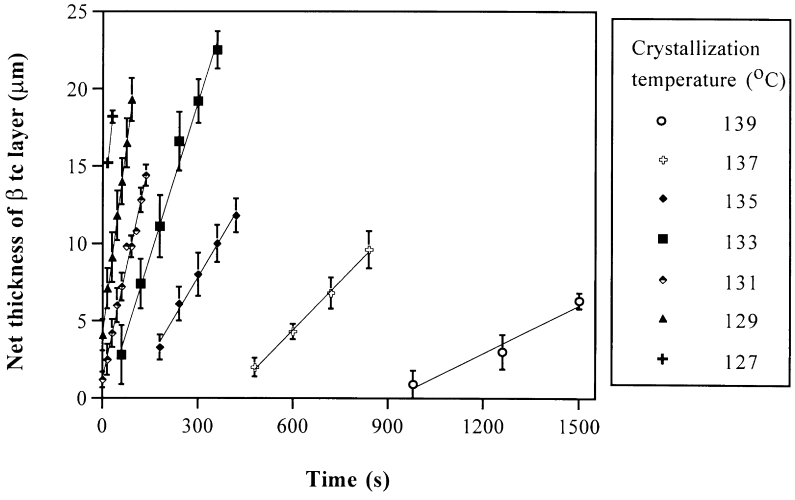

Fig. 16. Kinetics of β transcrystallization in GF/iPP.

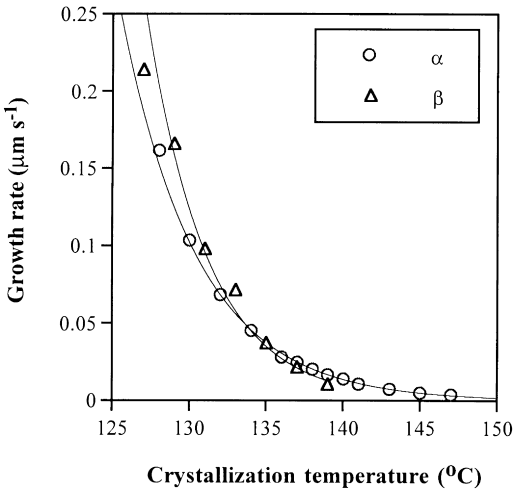

Fig. 17. The growth rates of α and β transcrystalline layers in iPP based composites.

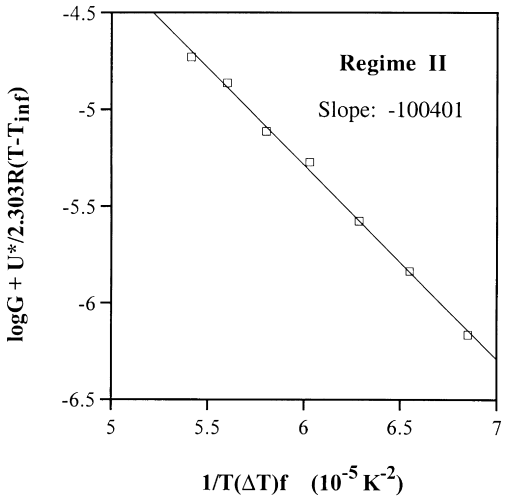

Fig. 18. A plot of log $G + U^*/2.303R(T - T_{inf})$ versus $1/T(\Delta T)f$ (according to Hoffman's theory) for the β transcrystalline layer in iPP-based composites.

slope of the HMCF/iPP data is outside the confidence interval for the slope of the iPP data at a low level of significance (around 50%), it is noted that other studies in the literature, such as of nylon 66 and its composites [24], report a similar tendency. Indeed higher activation energies for transcrystallization compared with bulk crystallization are expected due to the higher degree of order associated with the former. Thus, the degree of order is in the decreasing sequence: tc layers induced by KF, tc layers promoted by HMCF and bulk spherulites.

4.2. β Transcrystallization

β Transcrystallization of iPP can be induced either by coating a glass fibre with a specific nucleating agent (as in this work) or by inducing a shear stress in the matrix at the fibre–matrix interface [13]. However, a number of studies have shown that β iPP does not nucleate directly on the fibre surface. Rather, the β iPP interface grows always on top of a preceding thin α layer that nucleates initially on the fibre surface [13,14]. This phenomenon—termed bifurcation—implies that the nucleation of the β form is in fact not heterogeneous, leading to the occasional use of the term cylindritic structure instead of transcrystallinity. In this work, however, the term transcrystallinity is used exclusively because such an oriented layer will be obtained only if a fibre is inserted into the matrix. The whole interfacial region is considered a transcrystalline layer which is composed of two phases: the α and β crystalline forms.

The kinetics measurements of β transcrystallization could be performed only between 126 and 138°C because below 126°C, the bulk spherulites were too numerous and prevented the measurement of the tc layer radius. Above 138°C, no β phase crystallized and a pure α tc layer was obtained. Thus, interestingly, the kinetics measurements performed with this system extended the temperature range of regime II of α iPP and improved the accuracy of

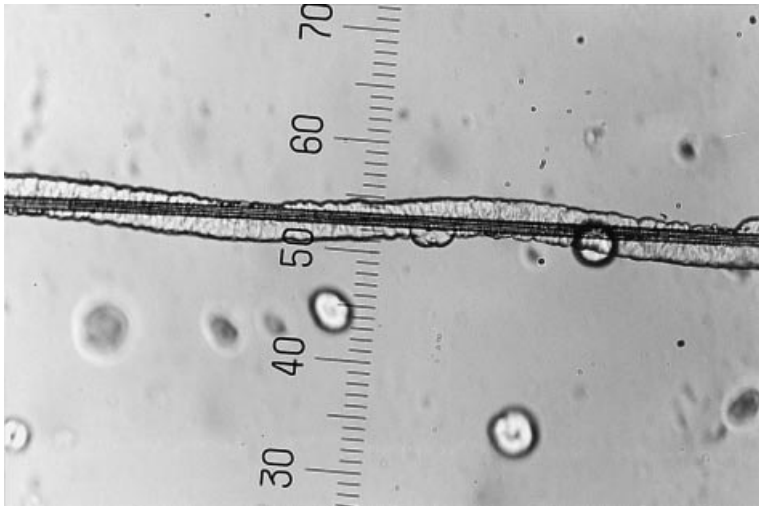

Fig. 19. A photograph of α transcrystalline layer grown on Kevlar 149 fibre, showing the typical helical formation.

the results (Fig. 6). Regarding the actual growth rate values of α and β tc layers, it is found that β transcrystallization is faster than α at lower temperature (up to 135°C, Fig. 17), as already shown for α and β spherulitic crystallization [19].

Regarding the effect of temperature on the number of nuclei and on their growth rates, the conclusions for β transcrystallization are the same as for α transcrystallization. In terms of Hoffman's model, the observed β transcrystallization is of regime II, with no regime transition within the investigated temperature range (Fig. 18). This is in agreement with results obtained for β spherulitic iPP, where a regime III–regime II transition has been observed at 123–129.5°C ($\Delta T = 46.5$–53°C) [19].

Finally, the induction time approach was not valid for β transcrystallization since the initial nucleation was always of the α form. Therefore it was impossible to evaluate the free energy difference at the interface between treated GF and iPP.

5. Conclusions

The kinetics of α and β transcrystallization in isotactic polypropylene based composites was investigated under isothermal treatment. The transcrystalline layer developed on glass fibres treated by a β nucleating agent was shown to be a mixture of α and β phase below 138°C. Above 138°C, the transcrystallinity was only of the α form.

The influence of nucleating fibres on the kinetics of α crystallization was as follows: whereas transcrystalline growth was not affected by the type of fibre and whereas the transition from regime III to regime II occured at the same temperature as for bulk spherulites, the significant difference between bulk crystallization and transcrystallization under isothermal conditions was manifested in the induction time. This parameter governs the final thickness of the transcrystalline layer and leads to the determination of the free energy difference functions. It was found that α crystallinity of iPP nucleates preferably on Kevlar 149 fibres than on high modulus carbon fibres and than in the bulk.

The thermal-gradient experiments resulted in the activation energy values. The activation energy was found to be higher for α transcrystallization than for α spherulitic crystallization, reflecting the higher ordered structure of the former.

Acknowledgements

The authors G.M. and H.D.W. acknowledge a financial support from the Israel Ministry of Science. This work was also supported in part by the Arc en Ciel-Keshet program, established by the French Embassy in Israel and the Israel Ministry of Science.

References

[1] Hoffman JD, Miller RL. Polymer 1997;38:3151.
[2] Hoffman JD. Polymer 1983;24:3.
[3] Ishida H, Bussi P. Macromolecules 1991;24:3569.
[4] Avella M, Volpe GD, Martuscelli E, Raimo R. Polym Engng Sci 1992;32:376.
[5] Thomason JL, Van Rooyen AA. J Mater Sci 1992;27:889.
[6] Wang C, Hwang L-M. J Polym Sci Part B: Polym Phys 1996;34:47.
[7] Wang C, Liu C-R. Polymer 1999;40:289.
[8] Incardona SD, Di Maggio R, Fambri L, Migliaresi C, Marom G. J Mater Sci 1993;28:4983.
[9] Fambri L, Incardona SD, Migliaresi C, Marom G. J Mater Sci 1994;29:4678.
[10] Klein N, Selivansky D, Marom G. Polym Compos 1995;16:189.
[11] Avella M, Martuscelli E, Selliti C, Garagnani E. J Mater Sci 1987;22:3185.
[12] Lustiger A, Marzinsky CN, Mueller RR, Wagner HD. J Adhes 1995;53:1.
[13] Varga J, Karger-Kocsis J. J Mater Sci Lett 1994;13:1069.
[14] Varga J, Karger-Kocsis J. Polym Commun 1995;39:4877.
[15] Assouline E, Fulchiron R, Gérard J-F, Wachtel E, Wagner HD, Marom G. J Polym Sci Part B: Polym Phys 1999;37:2534.
[16] Clark EJ, Hoffman JD. Macromolecules 1984;17:878.
[17] Hoffman JD, Davis GT, Lauritzen JI. Treatise on solid state chemistry, vol. 3. New York: Plenum Press, 1976 (chap. 7).
[18] Ishida H, Bussi P. In: Ishida H, editor. Controlled interphases in composite materials, New York: Elsevier, 1990. p. 391–9.
[19] Karger-Kocsis J. Polypropylene structure, blends and composites. 1st ed., vol. 1. London: Chapman and Hall, 1995 (chaps. 3 and 4).
[20] Tung CM, Dynes PJ. J Appl Polym Sci 1987;33:505.
[21] Lovinger AJ, Chua JO, Gryte CC. J Polym Sci Part B: Polym Phys 1977;15:641.
[22] Steenbakkers LW, Wagner HD. J Mater Sci Lett 1988;7:1209.
[23] Cheng SZD, Janimak JJ, Zhang A, Cheng HN. Macromolecules 1990;23:298.
[24] Klein N, Selivansky D, Marom G. Polym Compos 1995;16(3):189.